

OFFICE OF NAVAL RESEARCH

GRANT: N00014-93-1-0245

R&T Code: 4133041

Dr. Robert J. Nowak

Technical Report #3

Accession For	
NTIS	CRA&I <input checked="" type="checkbox"/>
DTIC	TAB <input type="checkbox"/>
Unannounced <input type="checkbox"/>	
Justification	
By	
Distribution/	
Availability Codes	
Dist	Avail and/or Special
A-1	

Morphology and Properties of Vanadium Oxide Xerogels and Aerogels

by

B. Katz*, W. Liu*, K. Salloux, F. Chaput, B. Dunn and G. C. Farrington*

Prepared for publication in the
Proceedings of the Materials Research Society Symposium on
Solid State Ionics

Department of Materials Science and Engineering
University of California, Los Angeles
Los Angeles, CA 90095-1595

*Department of Materials Science and Engineering
University of Pennsylvania
Philadelphia, PA 19104

July 14, 1995

Reproduction in whole, or in part, is permitted for any purpose
of the United States Government.

This document has been approved for public release and sale;
its distribution is unlimited.

19950720 036

AIRTEL

*Department of Materials Science and Engineering
University of California
Los Angeles CA 90024

The high redox potential and ion insertion properties of vanadium pentoxide have made this material a viable cathode for secondary lithium batteries. The use of sol-gel methods to synthesize vanadium pentoxide and other transition metal oxides has been well studied as the technique represents a relatively simple approach for preparing thin films and powders. Although it is well known that sol-gel processing may be used to prepare high surface area aerogels, the research on transition metal oxides has been largely limited to xerogels. The present paper compares the properties, structures and morphologies of vanadate xerogels and aerogels.

The sol-gel process is a wet chemical technique often used to synthesize oxide powders and glasses. In most cases the final product is formed by heat treating a gelled mixture of reactants, which drives off the gelled solvent and converts the gel into the desired form and composition, which is typically quite dense. When compared to conventional synthetic routes, sol-gel processing often has advantages such as lower sintering temperature, higher degree of purity, and greater product homogeneity.

Interestingly, more gentle methods of removing the solvent from a gel, such as simple air-drying at room temperature, freeze drying, or supercritical drying, can lead to quite intriguing new materials which have morphologies that not only retain the unusual gel microstructure but also possess their own distinctive characteristics. Air drying of gels generally produces hydrated oxide materials known as xerogels. Xerogels can be easily formed, via dipping or spinning methods, into thin film coatings having a variety of shapes and sizes. Supercritical drying of a gel can lead to the formation of aerogels, materials having exceptionally low densities, even lower than those of xerogels, and often formed as monoliths with extremely high surface areas.

The present paper compares and contrasts the microstructures, morphologies and properties of both xerogel and aerogel forms of vanadium oxides. The xerogels were prepared as thin films by the simple air drying of a vanadium oxide gel; whereas the aerogels were formed as monoliths by supercritical drying a vanadium oxide gel using CO_2 .

The sol-gel chemistry of vanadium oxide gels is well known [1-3]. In general there are two methods for preparing vanadate gels: the inorganic aqueous approach which makes use of proton exchange reactions with a sodium metavanadate solution and the organic alkoxide method [4]. In both cases the vanadate gel is comprised of a network of oxide fibers and water molecules. When the gel is dried in air, the oxide fibers tend to stack on top of each and prefer an orientation parallel to the substrate [5]. The xerogels thus formed are hydrous oxides; the amount of water present depends upon several factors such as humidity and the extent of reduced vanadium ions in the gel [6].

Vanadium oxide xerogels have a rich intercalation chemistry which includes reversible electrochemical lithium intercalation reactions. Lithium intercalation into the xerogels has been demonstrated by several groups [7-8]. However the chemistry of the intercalation is strongly dependent on the presence of solvent molecules between the layers and the age of the gel (V^{5+}/V^{4+} ratio). The high surface area and porosity of vanadium oxide aerogels makes them interesting candidates as high energy density battery electrodes [9]. Reversible electrochemical insertion of lithium ions into a vanadate aerogel is reported for the first time in this paper.

EXPERIMENTAL PROCEDURES

Method of Synthesis

Vanadium oxide gels were synthesized by both the widely-used ion exchange method and the alkoxide method [4]. Xerogel coatings were prepared by dip coating from gels derived by the ion exchange method. Monolithic vanadium oxide aerogels were prepared solely from alkoxide derived gels and were synthesized by supercritical drying with liquid CO_2 . The aerogel synthesis has been described in detail elsewhere [9]. Typical aerogel samples were prepared in the form of rods, 1 cm in diameter by 3 cm in length.

Characterization

Thermogravimetric analysis (TGA) was carried out using a DuPont 9900 Thermal Analysis System. The weight loss upon heating was measured from 25°C to temperatures as high as 500°C at heating rates of 5°C/min and 10°C/min in nitrogen.

X-ray diffraction patterns were obtained on a Rigaku diffractometer using $Cu\ K\alpha$ radiation. Xerogel coatings were prepared on glass slides for reflection mode x-ray diffraction experiments and on cleaved mica for transmission mode x-ray diffraction experiments. Aerogel diffraction experiments (reflection mode geometry) were performed on large aerogel fragments and aerogel powders. Scanning electron microscopy (SEM) experiments were performed on aerogel fragments and xerogel coatings. An investigation of the cross section of a xerogel coating was also performed using the SEM. The cross sections were exposed by cracking a xerogel coated glass slide in liquid nitrogen. The SEM used in the study was a high resolution JEOL 6300FV.

Electrochemical cells were prepared inside an argon filled dry box. The electrolyte used was a 1M lithium perchlorate in propylene carbonate. The lithium perchlorate salt was first heated in a vacuum oven for 24 hours at 120°C. The propylene carbonate was dried over activated molecular sieves for 5 days. The xerogel samples were all prepared on platinum substrates. The vanadate aerogel samples were crushed into a powder, mixed with cyclopentanone and spun onto molybdenum-coated glass slides. Lithium foil was used for the counter and reference electrodes. Prior to electrochemical experiments the

xerogel coatings were placed in the electrolyte for at least 24 hours. The cyclic voltammetry experiments were performed at a scanning rate of 1mV/sec. The potentiostat used was a PAR 273A.

MIRIS

RESULTS

Chemical Properties

Vanadate aerogels had surface areas in the range of 300 to 400 m²/g and pore volumes as large as 1.5 cm³/g. The density of the aerogel was as low as 0.04 g/cm³ to 0.1 g/cm³, which corresponds to a solid content of 1% to 3%.

Thermogravimetric analysis of xerogel coatings indicated the existence of at least 1.6 moles of water per mole of oxide (assuming V₂O₅ as the solid phase). The weight change profile for the xerogel is characterized by a steep loss between room temperature and 100°C, followed by a more gradual weight loss up until 300°C, at which point there is a sharp 5% weight loss; see Figure 1a. In comparison, TGA results for the aerogel indicate at least 2.2 moles of water per mole of oxide (assuming V₂O₅ as the solid phase). The weight change profile of the aerogel is analogous to that of the xerogel except that there is no indication of a sharp water loss at temperatures around 300°C, Figure 1b.

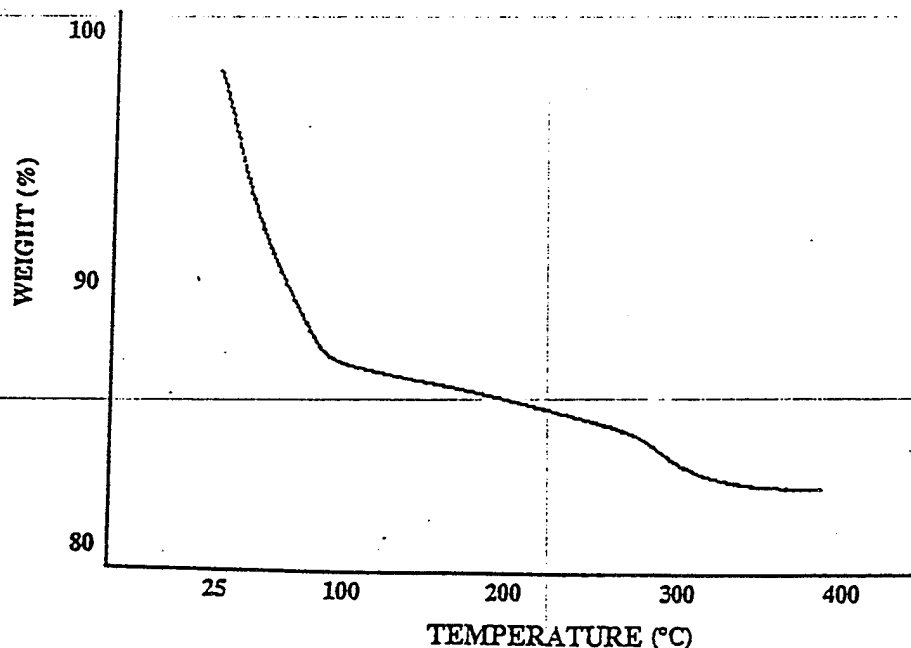


Figure 1a. TGA scan for xerogel. The sample was heated at a rate of 5°C per minute in a nitrogen atmosphere

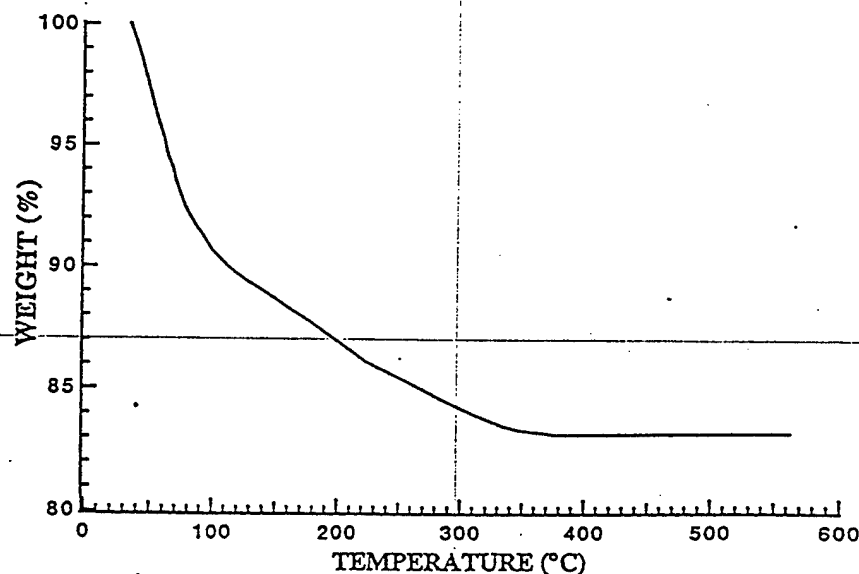


Figure 1b. TGA scan for aerogel. The sample was heated at a rate of 10°C per minute in a nitrogen atmosphere

X-Ray Diffraction

The reflection mode x-ray diffraction pattern of a vanadium oxide xerogel coating is typical of a layered structure having a preferred orientation, Figure 2a. All the diffraction peaks can be indexed as 00l harmonics, the average inter-layer spacing being 11.6Å. The extent of the preferred orientation in the xerogel coating is illustrated by its rocking curve, Figure (3), the halfwidth of which is 17°. The transmission mode diffraction pattern of the xerogel coating is completely different from that of the corresponding reflection mode diffraction pattern, Figure 2b. Considering the turbostratic structure of the xerogel, all the peaks in the transmission pattern have been indexed as hk reflections [5].

All the peaks present in the reflection mode diffraction pattern of the aerogel are observed in the combined reflection and transmission mode diffraction patterns of a xerogel coating, Figure 2c. The peak position of the 001 reflection occurs at a 2θ angle greater than that of the xerogel, indicating a larger layered spacing for the aerogel. Moreover, the aerogel material does not show any degree of preferred orientation.

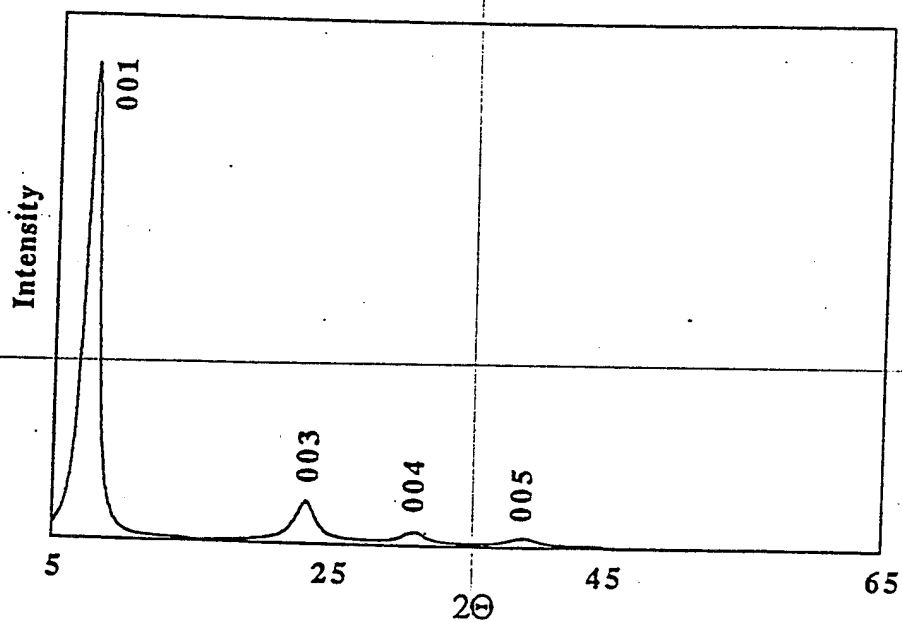


Figure 2a. Reflection mode X-ray diffraction pattern of a xerogel.

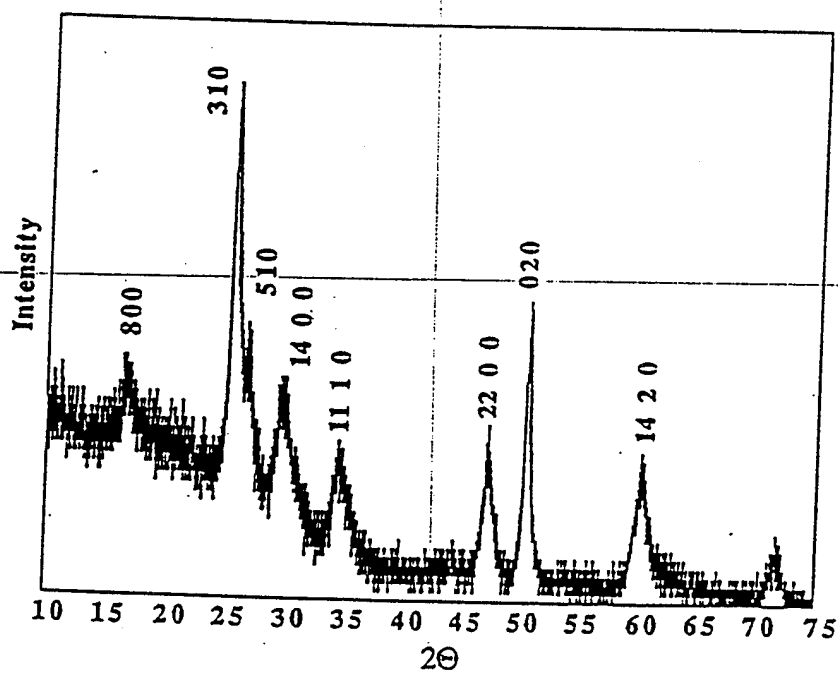


Figure 2b. Transmission mode X-ray diffraction pattern of a xerogel coating.

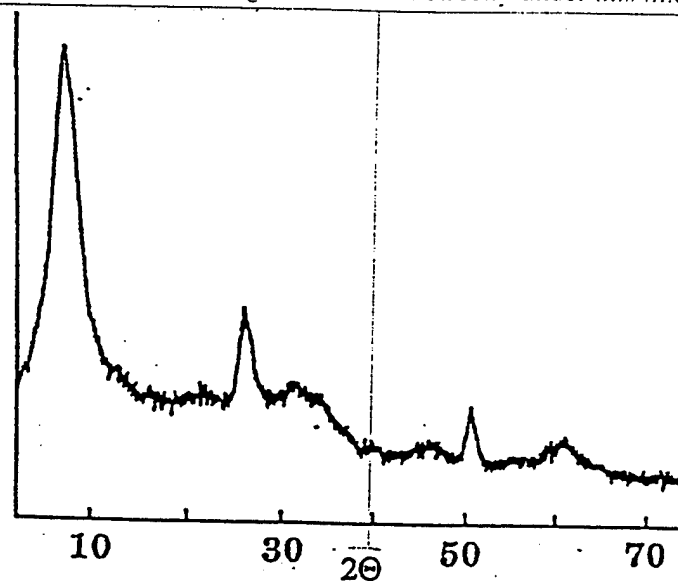


Figure 2c. Reflection mode X-ray diffraction pattern of an aerogel

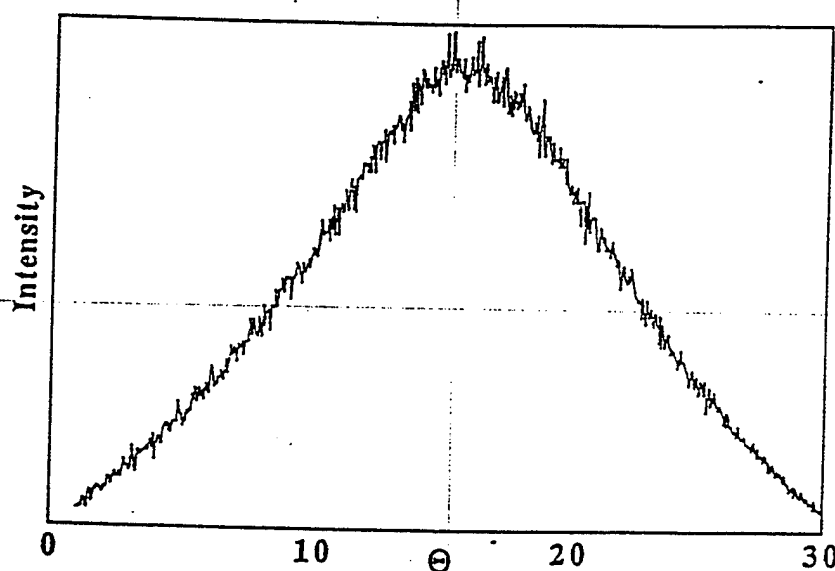


Figure 3. Rocking curve of a vanadate xerogel coating; less than 1 μm thick.

Scanning Electron Microscopy

TEM investigations of the vanadate aerogel reveal the fibrous nature of its microstructure [9]. The ribbon-like structure of these fibers is similar to what is observed with vanadate xerogels [5].

An SEM micrograph of a dip coated xerogel is shown in Figure 4a. The texture of the coating shows evidence of a complex folding in what appears to be a homogeneous and corrugated morphology. The SEM micrograph in Figure 4b shows the cross section of a xerogel coating. The lamellar nature of the xerogel and its high porosity are evident in the micrograph. In comparison, the aerogel morphology appears to take the form of an interwoven network of oxide fibers, Figure 5. The low density and extremely high porosity of the aerogel are clearly seen in the micrograph.

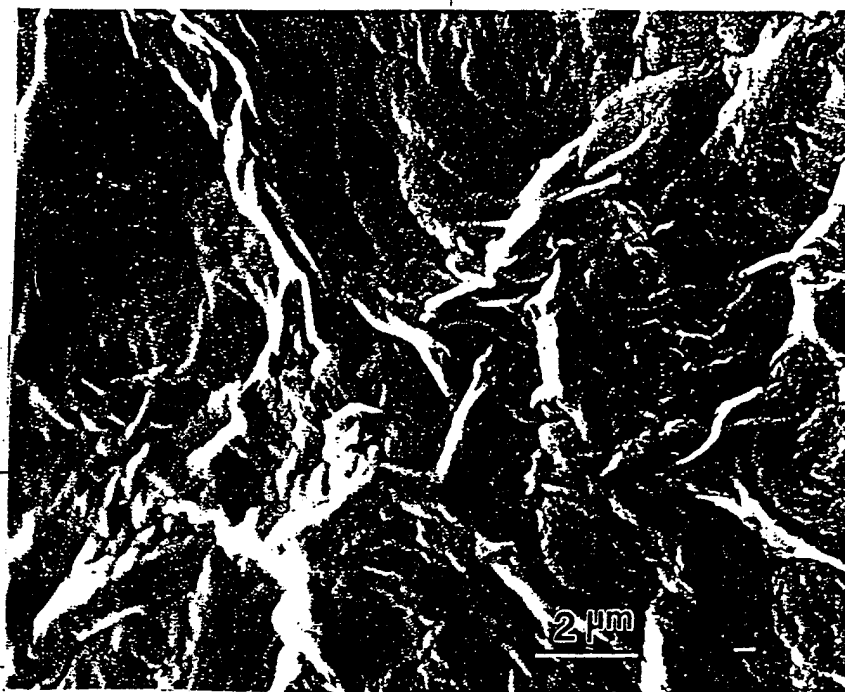


Figure 4a. SEM micrograph of the surface of a xerogel coating

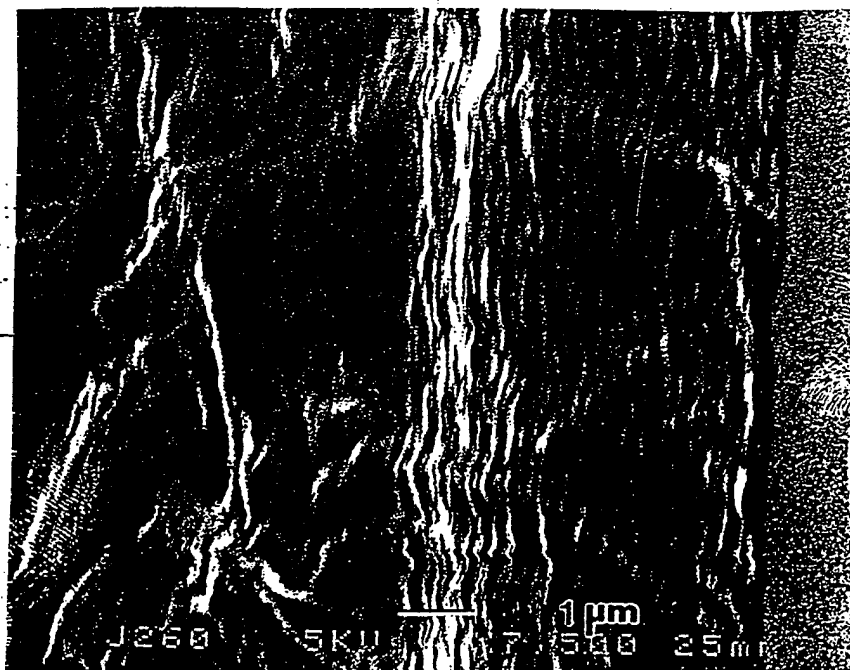


Figure 4b. SEM micrograph of a cross section of a xerogel coating

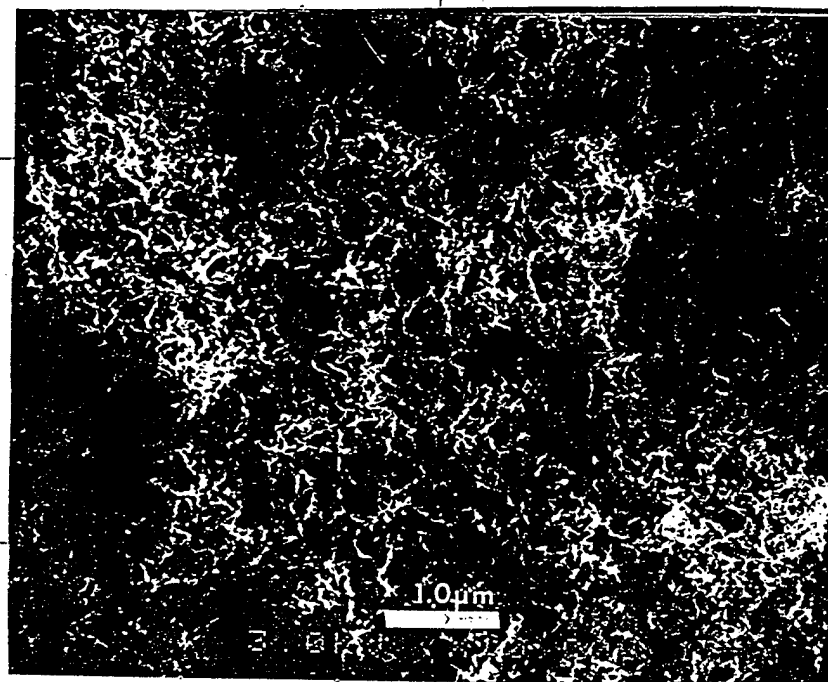


Figure 5. SEM micrograph of an aerogel fragment.

Electrochemical Lithium Intercalation

Figure 6a is a cyclic voltammogram of a xerogel coating (red in color) that, prior to electrochemical reduction, had undergone swelling of its layers by propylene carbonate molecules. The swelling was confirmed by x-ray diffraction experiments that showed the inter-layer distance increased from 11.6Å to 20.9Å. The cyclic voltammogram in Figure 6a exhibits a single broad cathodic and a single broad anodic peak centered around 2.8 volts and 3.4 volts respectively.

Figure 6b is a cyclic voltammogram of an aerogel that was crushed into powder form. In contrast to the broad reduction peaks observed with the red xerogel, the cyclic voltammogram of the aerogel exhibits two cathodic peaks around 2.9 volts and 2.4 volts. Moreover, both reduction peaks appear to ride on top of a single broad cathodic peak. The anodic wave of the cycle, corresponding to de-intercalation of lithium ions, gives rise to a single and relatively sharp peak at 3.5 volts.

MIRIS

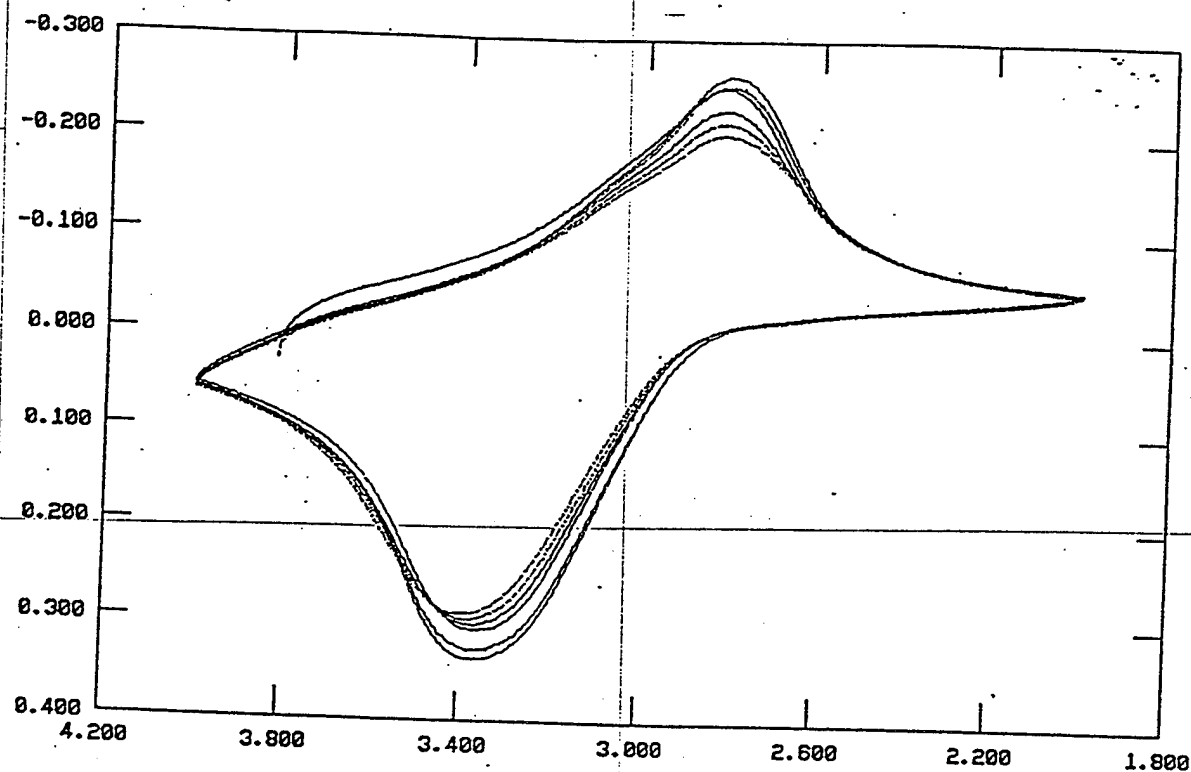


Figure 6a. Cyclic voltammogram of a fresh xerogel coating undergoing reversible lithium intercalation

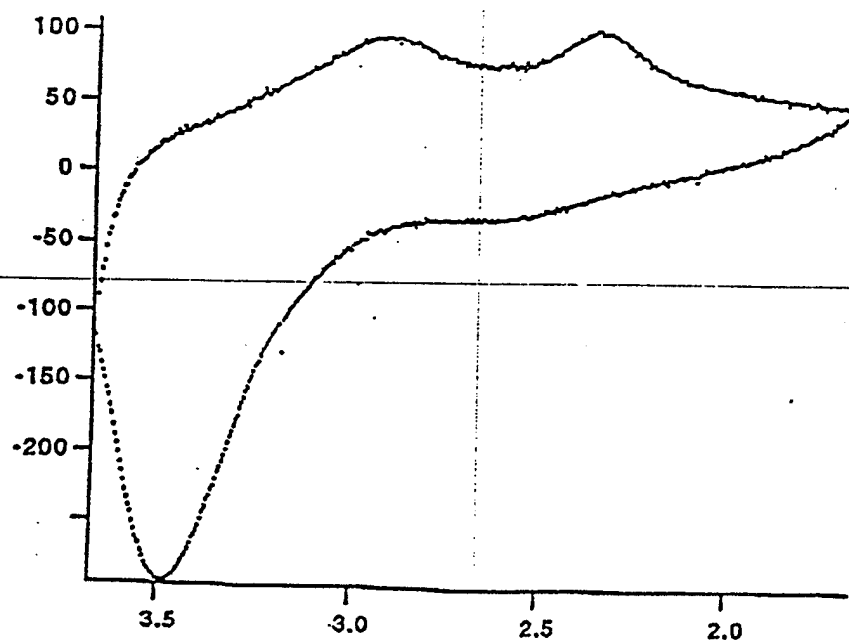


Figure 6b. Cyclic voltammogram of an aerogel undergoing reversible lithium intercalation

DISCUSSION

The various techniques used to examine the structure of vanadate xerogel films prepared by dip coating and drying show that the films consist of ribbon-like vanadium oxide layers laid on top of each other with preferred orientation parallel to the substrate. Although the preferred orientation is not perfect, as shown by the rocking curve, it is complete enough to prevent the appearance of any reflections other than 00l in a reflection mode diffractogram. Thus, vanadium oxide xerogels have a random layer structure that arises from a stacking of the oxide layers parallel to one another but with mis-registry between the layers about the layer normal [5]. The absence of layer-to-layer registry prevents the appearance of general hkl reflections. However the individual layers diffract independently, giving rise to two dimensional hk reflections. As a result of the preferred orientation of the layers in a xerogel coating the only reflections observed in its transmission x-ray diffraction pattern are of the hk type. The hk reflections, which have been indexed based on the electron diffraction investigations of Kittaka et al. [10], do not correspond to any known vanadium oxides.

The x-ray diffraction pattern of an aerogel is quite similar to the combined reflection and transmission mode diffraction patterns of a xerogel coating. All the peak positions except the 001 are the same, indicating that there is no preferred orientation among the aerogel fibers and that the atomic structure of the individual layers in the aerogel is similar to that of the xerogel layers. The 001 peak in the aerogel diffractogram corresponds to a layer separation of about 12.7Å, compared to 11.6Å for the xerogel. The larger spacing is most likely the result of the increased level of hydration of the aerogel ($n=2.2$) compared to that of the xerogel ($n=1.6$). In fact it has previously been shown that the hydration state of xerogels strongly depends on their reduction state [5]. The aerogels, which are dark green in color, are partially reduced during synthesis. The larger degree of hydration of the aerogels may well be explained by the greater state of reduction as compared to that of a fresh xerogel. In addition, the absence of any 00l harmonics with $n>1$ in the aerogel diffractogram is most likely due to low diffraction intensities resulting from both a lack of preferred orientation and small coherence lengths between diffracting layers.

The corrugated morphology of the xerogel coating as seen in the SEM micrograph of Figure 4a is most likely the result of shrinkage as the gel dries. Furthermore the lamellar nature of the xerogel, which is unmistakably evident in the cross section shown in Figure 4b, most probably arises because of the preferred stacking of the layers. In comparison, aerogel morphologies appear to resemble the oxide skeleton of the starting gel phase; see Figure 5. In this way the aerogel may be considered as the rigid oxide skeleton that corresponds to the solid matrix that exists in the hydrated gel. It appears that the supercritical drying process removes the solvent but leaves the solid relatively intact.

The TGA curves for xerogels and aerogels are quite similar, except for the amount of water per mole of oxide and the lack of any sharp weight loss for the aerogel around 300°C; see Figures 1a and 1b. It is well established that vanadate xerogels undergo a sharp weight loss of approximately 5% at 300°C prior to their transformation to crystalline V_2O_5 . Curiously, there is no analogous weight loss from vanadate aerogels prior to the formation of crystalline V_2O_5 . We are presently carrying out in-situ x-ray diffraction experiments as a function of temperature in an attempt to understand these differences. As mentioned earlier, the larger hydration state of the aerogel ($n=2.2$) relative to that of a fresh xerogel ($n=1.6$) is likely the result of a greater degree of reduction in the aerogel.

The electrochemistry of vanadate xerogels has been investigated in a number of laboratories over the last decade. The ease of sample preparation and fabrication into thin films, along with the high oxidation potential of the vanadate xerogels, are reasons why they are considered by some to be attractive electrode materials. Unfortunately, the complicated chemistry of the xerogel has made it difficult to characterize completely the lithium intercalation process.

It is clear that the Li^+ intercalation chemistry of the vanadate xerogels is strongly affected by the presence or absence of neutral molecules (e.g. water, propylene carbonate, polymers) intercalated between the oxide layers [11]. Figure 6a shows a typical cyclic voltammogram of a xerogel coating in which propylene carbonate molecules had been intercalated into the lamellar spaces. It is characterized by broad cathodic and anodic peaks. In contrast we have shown previously that xerogels that do not undergo PC insertion prior to lithium intercalation have cyclic voltammograms exhibiting three intercalation and de-intercalation peaks, all of which ride on top of a broad peak [11].

Vanadate aerogels also undergo reversible lithium intercalation, as shown in the cyclic voltammogram in Figure 6b. The cathodic portion of the curve is somewhat similar to that of an aged xerogel, exhibiting two peaks riding on top of a rather broad peak. Curiously, the anodic portion of the cyclic voltammogram exhibits only a single sharp peak at 3.5 volts, indicating that the de-intercalation process occurs in a single step.

CONCLUSIONS

The microstructure, morphology and properties of sol-gel derived vanadate xerogels and aerogels are quite intriguing. The fibrous nature of the vanadate gel phase is retained in both, though their respective morphologies are quite different. The slow drying of the gel during xerogel formation gives rise to a lamellar texture in which the oxide fibrils have a preferred orientation parallel to the substrate on which the xerogel is deposited. In contrast, the rapid supercritical drying process by which the aerogel is formed removes the solvent phase so quickly that the three-dimensional solid oxide matrix of the gel appears to be frozen in place. Vanadate aerogels undergo reversible Li^+ intercalation by reactions that appear similar to those of an aged xerogel coating.

ACKNOWLEDGEMENTS

This work was performed under financial support given by the Office of Naval Research through the grant DMR-14-90-5-1156 and the National Science Foundation, MRL program, under grant No.DMR 91-20668.

The authors would also like to thank K. Kowal for his assistance, as well as X.Q. Wang and Dr. R. Lakis for their help regarding the scanning electron microscopy studies.

REFERENCES

1. J. Lermerle, L. Nejem and J. Lefebvre, J. Chem. Res., Miniprint. 5, 301 (1978).
2. J. Lermerle, L. Nejem and J. Lefebvre, J. Inorg. Nucl. Chem. 42, 17 (1980).
3. J. Livage, Chem. Mater. 3, 578 (1991).
4. J. Livage, M. Henry and C. Sanchez, Prog. Solid. St. Chem. 18, 259 (1988).
5. P. Aldebert, N. Baffier, N. Gharbi and J. Livage, Mater. Res. Bull. 16, 669 (1981)
6. J. Livage, Mater. Res. Bull. 26, 1173 (1991).
7. K. West, B. Zachau-Christiansen, T. Jacobsen and S. Skaarup. Electrochim. Acta. 38, 1215 (1993)
8. R. Baddour, J.P. Pereira-Ramos, R. Messina and J. Perichon. J. Electroanal. Chem. 314, 81 (1991)
9. F. Chaput, B. Dunn, P. Fuqua and K. Salloux. J. Non-Crystal. Solids. (to be published)
10. S. Kittaka, N. Uchida, H. Miyahara and Y. Yokota, Mat. Res. Bull. 26, 391 (1991)
11. B. Katz, R. Huq and G.C. Farrington, Solid State Ionics. (to be published)

REPORT DOCUMENTATION PAGE

Form Approved
OMB No. 0704-0188

Public reporting burden for this collection of information is estimated to average 1 hour per response, including the time for reviewing instructions, searching existing data sources, gathering and maintaining the data needed, and completing and reviewing the collection of information. Send comments regarding this burden estimate or any other aspect of this collection of information, including suggestions for reducing this burden, to Washington Headquarters Services, Directorate for Information Operations and Reports, 1215 Jefferson Davis Highway, Suite 1204, Arlington, VA 22202-4302, and to the Office of Management and Budget, Paperwork Reduction Project (0704-0188), Washington, DC 20503.

1. AGENCY USE ONLY (Leave blank)

2. REPORT DATE
July 14, 1995

3. REPORT TYPE AND DATES COVERED
Technical Report 06/01/94 - 05/31/95

4. TITLE AND SUBTITLE

Morphology and Properties of Vanadium Oxide Xerogels and Aerogels

5. FUNDING NUMBERS

Grant: N00014-93-1-0245
Dr. Robert J. Nowak
R&T Code: 4133041

6. AUTHOR(S)

B. Katz, W. Liu, K. Salloux, F. Chaput, B. Dunn and G.C. Farrington

7. PERFORMING ORGANIZATION NAME(S) AND ADDRESS(ES)

Department of Materials Science and Engineering
University of California, Los Angeles
Los Angeles, CA 90095-1595

8. PERFORMING ORGANIZATION
REPORT NUMBER

Technical Report No. 3

9. SPONSORING/MONITORING AGENCY NAME(S) AND ADDRESS(ES)

Office of Naval Research
Chemistry Division
800 North Quincy Street
Arlington, VA 22217-5660

10. SPONSORING/MONITORING
AGENCY REPORT NUMBER

11. SUPPLEMENTARY NOTES

For publication in Proc. Materials Research Society Symposium on Solid State Ionics

12a. DISTRIBUTION/AVAILABILITY STATEMENT

This document has been approved for public release and sale; its distribution is unlimited.

12b. DISTRIBUTION CODE

13. ABSTRACT (Maximum 200 words)

The high redox potential and ion insertion properties of vanadium pentoxide have made this material a viable cathode for secondary lithium batteries. The use of sol-gel methods to synthesize vanadium pentoxide and other transition metal oxides has been well studied as the technique represents a relatively simple approach for preparing thin films and powders. Although it is well known that sol-gel processing may be used to prepare high surface area aerogels, the research on transition metal oxides has been largely limited to xerogels. The present paper compares the properties, structures and morphologies of vanadate xerogels and aerogels.

DTIC QUALITY INSPECTED 5

14. SUBJECT TERMS

Vanadium pentoxide, xerogel, aerogel, microstructure

15. NUMBER OF PAGES

12

16. PRICE CODE

17. SECURITY CLASSIFICATION
OF REPORT

Unclassified

18. SECURITY CLASSIFICATION
OF THIS PAGE

Unclassified

19. SECURITY CLASSIFICATION
OF ABSTRACT

Unclassified

20. LIMITATION OF ABSTRACT